Coherence and curvature attributes on preconditioned seismic data

Satinder Chopra and Somanath Misra, Arcis Corporation, Calgary
Kurt J. Marfurt, University of Oklahoma

Seismic data are usually contaminated with both random and coherent noise, even when the data have been properly migrated and are multiple-free. Seismic attributes are particularly effective at extracting subtle features from relatively noise-free data. Certain types of noise can be addressed by the interpreter through careful structure-oriented filtering or postmigration footprint suppression. However, if the data are contaminated by multiples or are poorly focused and imaged due to inaccurate velocities, the data need to go back to the processing team.

Another common problem with seismic data is their relatively low bandwidth. Significant efforts are made during processing to enhance the frequency content of the data as much as possible to provide a spectral response that is consistent with the acquisition parameters. Ironically, the interpreters can be somewhat more aggressive in their filtering. The interpreters will have a better understanding of the play concept, access to any well data, and therefore be better able to keep or reject alternative filter products that are consistent or inconsistent with the interpretation hypothesis.

We begin our discussion by reviewing alternative means of suppressing random noise on our migrated seismic images, with the most promising methods being various implementations of structure-oriented filtering. Next, we address acquisition footprint, which may appear to be random in the temporal domain but is highly correlated to the acquisition geometry in the spatial domain. After running the data through the cleaning phase, we evaluate alternative methods for frequency enhancement of the input seismic data. We illustrate the impact of these preconditioning steps on the computation of the attributes such as coherence and curvature on data volumes from Alberta, Canada. We conclude with a summary on the choice of the frequency-enhancement methods on the basis of the examples generated with different workflows.

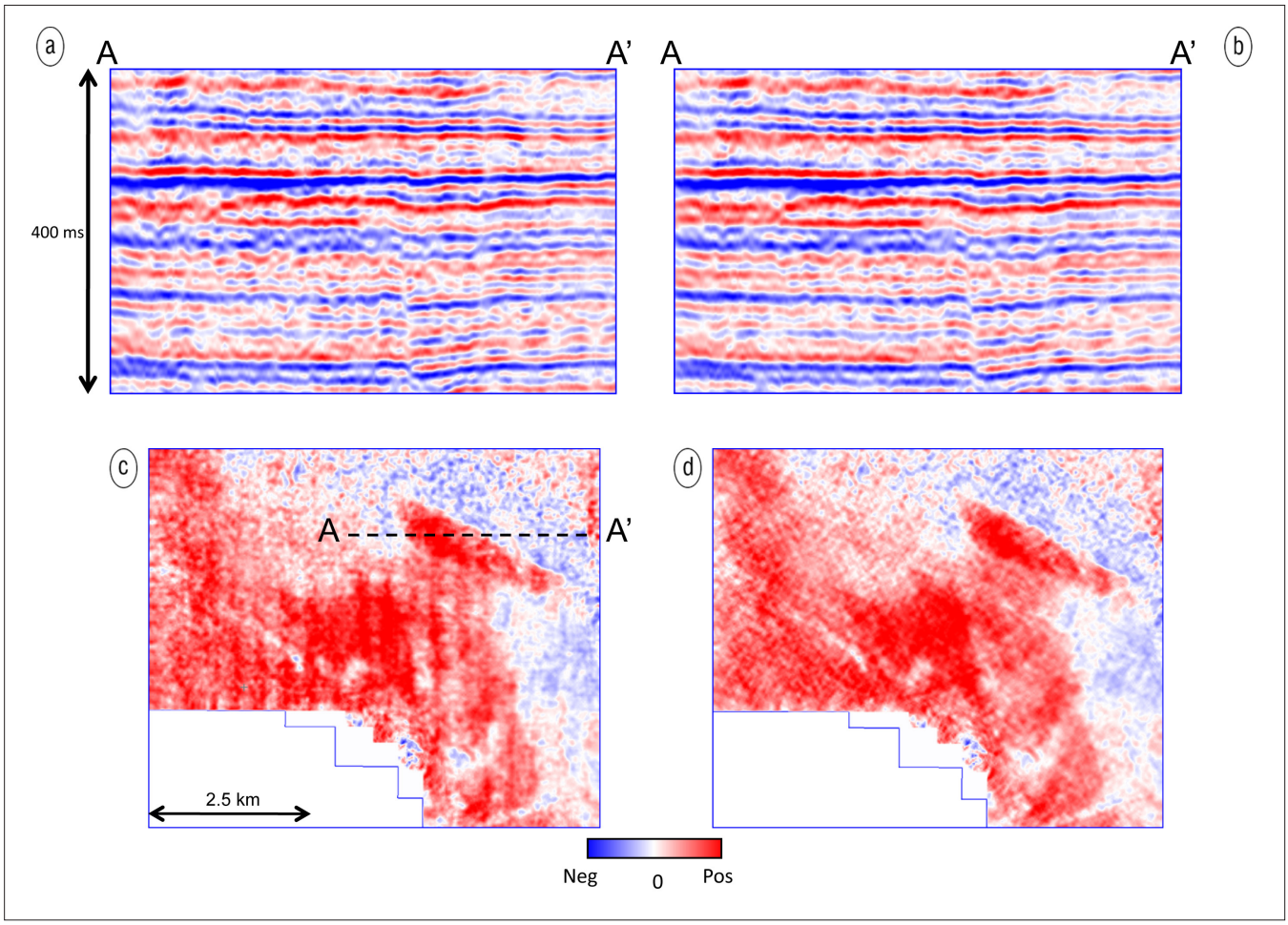

Figure 1. *Vertical slice AA' through a seismic amplitude volume (a) before and (b) after* k_x-k_y *filtering to suppress acquisition footprint. Time slices at t = 769 ms (c) before and (d) after* k_x-k_y *filtering. Notice the removal of the NS imprint seen in (c) on the filtered results in (d).*

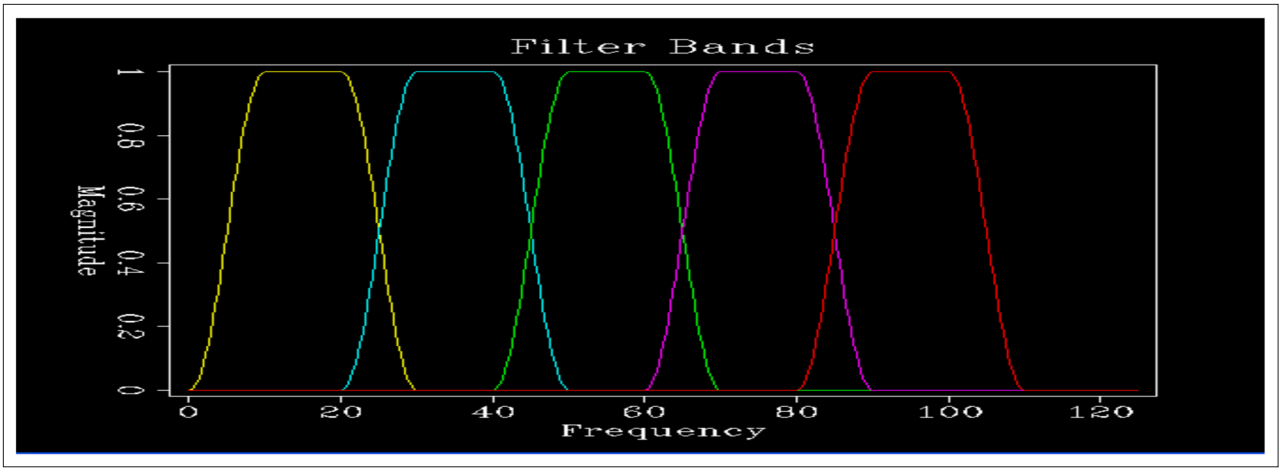

Figure 2. *Passbands used in frequency-split structure-oriented filtering. Each band-passed seismic data volume is subjected to principal-component structure-oriented filtering, then normalized to the amplitude of the original spectrum before reassembling the result.*

Alternative noise-suppression workflows

Suppression of random noise: Mean, alpha-trimmed mean, and median filters are commonly used during processing to suppress random noise. A more desirable application would be of a dip-steered mean or median filter, which has the effect of enhancing laterally continuous events by reducing randomly distributed noise without suppressing details in the reflection events consistent with the structure. The filter picks up samples within the chosen aperture along the local dip and azimuth and replaces the amplitude of the central sample position with the median value of the amplitudes. The median filter can also be applied iteratively, reducing random noise at each successive iteration, but will not significantly increase the high frequency geological component of the surface (Chopra and Marfurt, 2008).

Dip-steered mean filters work well on prestack data in which discontinuities appear as smooth diffractions, but smear faults and stratigraphic edges on migrated data. Dip-steered median and alpha-trimmed mean filters work somewhat better but will still smear faults. Hoecker and Fehmers (2002) address this problem through an "anisotropic diffusion" smoothing algorithm. The anisotropic part is so named because the smoothing takes place parallel to the reflector, while no smoothing takes place perpendicular to the reflector. The diffusion part of the name implies that the filter is applied iteratively, much as an interpreter would apply iterative smoothing to a time-structure map. Most important, no smoothing takes place if a discontinuity is detected, thereby preserving the appearance of major faults and stratigraphic edges. Luo et al. (2002) proposed a competing method that uses a multiwindow (Kuwahara) filter to address the same problem. Both approaches use a mean or median filter applied to data values that fall within a spatial analysis window with a thickness of one sample.

Marfurt (2006) describes a multiwindow (Kuwahara) principal component filter that uses a small volume of data samples to compute the waveform that best represents the seismic data in the spatial analysis window. Seismic processors may be more familiar with the principal component filter as equivalent to the Kohonen-Loeve (or simply KL) filter commonly used to model and remove multiples on NMO-corrected gathers using the multiple velocity. Examples of the application of structure-oriented filtering on seismic data have been shown in Chopra and Marfurt (2007, 2008a, 2008b), wherein improved event focusing and reduced background noise levels after structure-oriented filtering are clearly evident.

Suppression of acquisition footprint: Acquisition footprint is defined as any amplitude or phase anomaly closely correlated to the surface acquisition geometry rather than to the subsurface geology. Most acquisition is based on a live source-receiver path that is repeated laterally to span the entire sur-

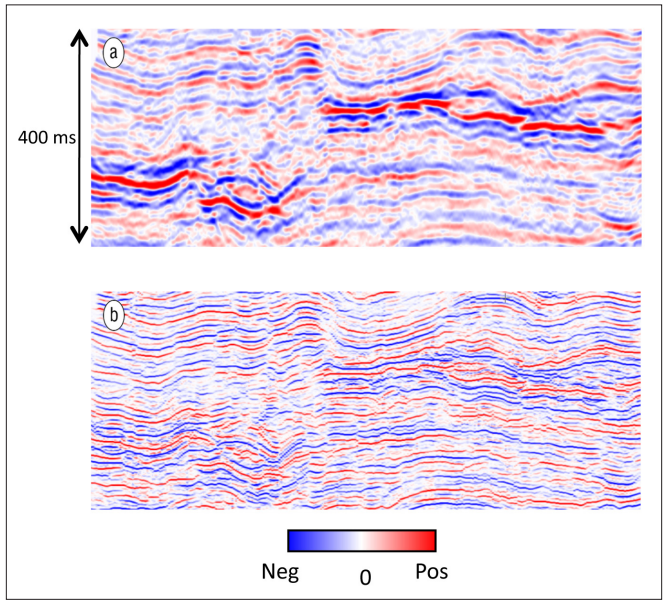

Figure 3. *(a) A segment of a seismic section and (b) equivalent thin-bed reflectivity section derived from the input section. Notice the higher resolution as well the extra cycles that help make a more accurate interpretation.*

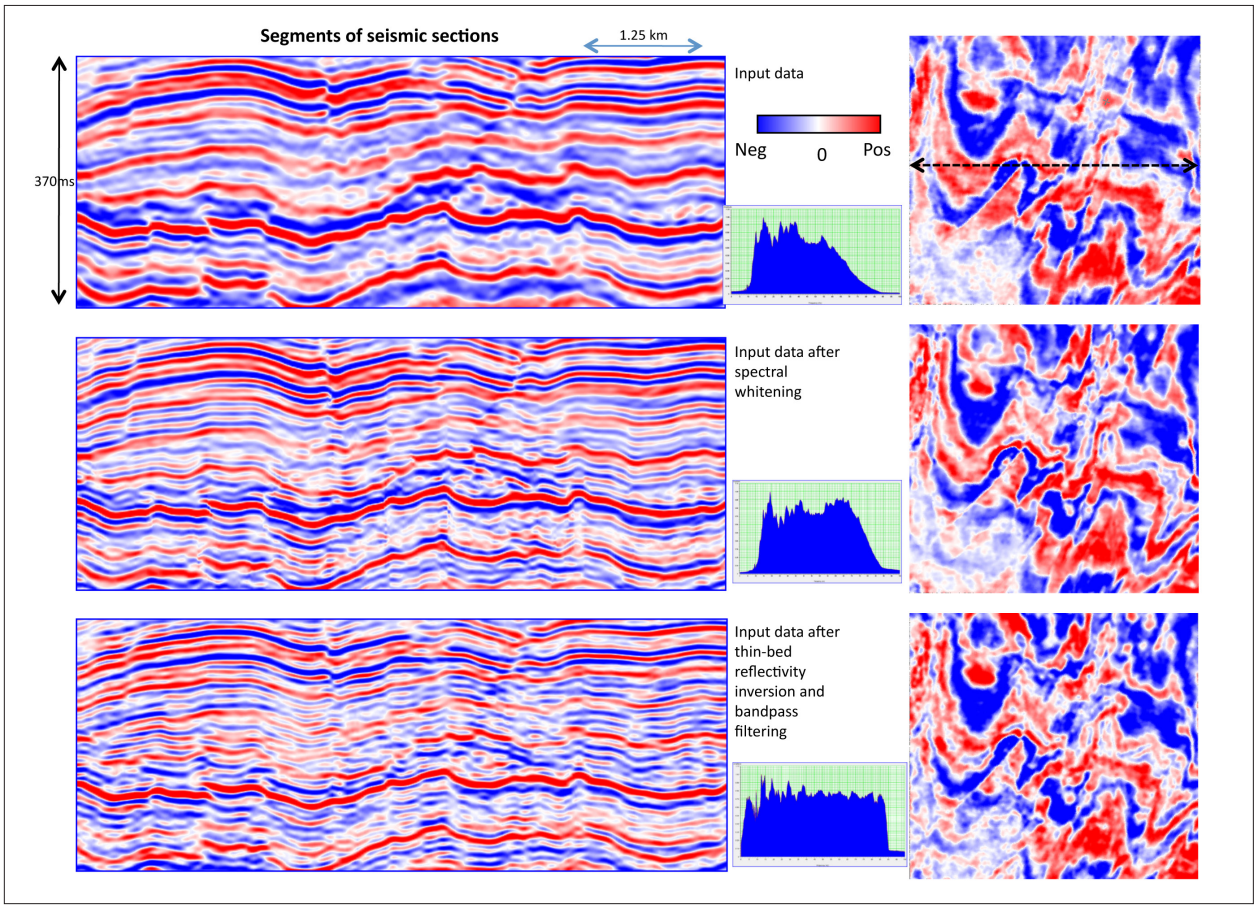

Figure 4. *A seismic section and a time slice (1140 ms) from (a) input data volume, (b) the same data as in (a) after time-variant spectral whitening, and (c) the same data in (a) after thin-bed reflectivity inversion. Notice the enhancement in reflection detail on the vertical as well as on the time sections after TVSW and thin-bed reflectivity inversion. The amplitude spectrum shown for each data set indicate thin-bed reflectivity detail yielding higher frequency enhancement than TVSW.*

vey area, resulting in spatially periodic changes in total fold, azimuths, and offsets which in turn give rise to spatial periodicity in signal-to-noise ratio, AVO response, and moveout errors. Attributes exacerbate these periodic changes, giving rise to artifacts. Gulunay (2006) and others have shown that k_x-k_y filters can be effective in reducing acquisition footprint on time slices for regularly sampled surveys. Because footprint due to fold, offset, and azimuth tends to be organized vertically, while that due to aliased migration artifacts is steeply dipping, k_x-k_y-w or 3D running-window Radon filters may provide some additional artifact-suppression leverage. For more irregular acquisition design, the noise estimated using k_x-k_y or k_x-k_y-w filters can be followed by an adaptive filter.

Figures 1a and 1b compare a segment of a seismic section before and after footprint suppression. The vertical section in Figure 1a exhibits the short wavelength jitter common to acquisition footprint, which is diminished after k_x-k_y filtering. Figures 1c and 1d show the effect seen on time slices at t=769 ms through the two amplitude volumes. Notice the moderate wavelength NS imprint masking the time slice in Figure 1c which is suppressed after k_x-k_y filtering in Figure 1d.

Enhancing the spectral bandwidth of seismic data

There are a number of methods that are used during processing to enhance the frequency content of the input seismic data. Here we mention a few commonly used processes followed by some relatively newer ones that help the interpreter extract meaningful information from the seismic data.

Deconvolution: Different conventional procedures are adopted to compensate for frequency attenuation. A common practice has been to use a two- or three-window statistical deconvolution to correct for the dynamic loss of high frequencies with increasing traveltime. This involves choosing two or three time windows for the deconvolution, each with its own parameters, keeping the time-variant nature of the embedded source wavelet in mind. These windows overlap to avoid artifacts. However, problems can arise because the filters are now derived from smaller windows, which are less likely to meet the statistical assumptions made in constructing the deconvolution operator, often resulting in phase distortions at the point of overlap.

Time-variant spectral whitening: The other method is to use time-variant spectral whitening (TVSW). The method involves passing the input data through a number of narrow band-pass filters and determining the decay rates for each frequency band. The inverse of these decay functions for each frequency band is applied and the results are summed. In this way, the amplitude spectrum for the output data is whitened

in a time-variant way. The number of filter bands, the width of each band and the overall bandwidth of application are the different parameters that are used and adjusted for an optimized result (Yilmaz 2001). In this method, the high-frequency noise is usually amplified and so a band-pass filter must be applied to the resulting data. Because it is a trace-by-trace process, TVSW is not appropriate for AVO applications.

Inverse Q-filtering: If we had an analytic form for an attenuation function, it would then be easy to compensate for its effects. Typically a constant Q-model is assumed. In addition to compensating for absorption by boosting the amplitude of the higher frequency components, an accurate inverse Q-filter will also compensate for the corresponding dispersion effects by rotating the phase components of seismic data. Inverse Q-filtering is most successful when combined with direct VSP measurements of waveform attenuation and dispersion. Good results can also be obtained by generating a suite of time-varying wavelets correlated to good well control. Statistical estimates of Q from surface seismic data alone have proven to be more challenging.

Frequency split structurally oriented filtering: Helmore (2009) introduced frequency split structurally oriented filtering (Figure 2) wherein the input seismic data are divided into a number of frequency bands, followed by running structurally oriented filters separately to each of the bands and then recombining the results. This procedure reduces noise in selected frequency bands and results in higher signal-to-noise ratio as well as enhanced resolution. Structurally oriented filters do not suffer from windowing artifacts and are precisely adapted to the local dip (Helmore, 2009).

Spectral decomposition-based inversion for seismic reflectivity: Thin-bed spectral inversion (Chopra et al., 2006) is a process that removes the time-variant wavelet from the seismic data and extracts the reflectivity to image thicknesses far below seismic resolution using a matching-pursuit variant of sparse spike inversion. In addition to enhanced images of

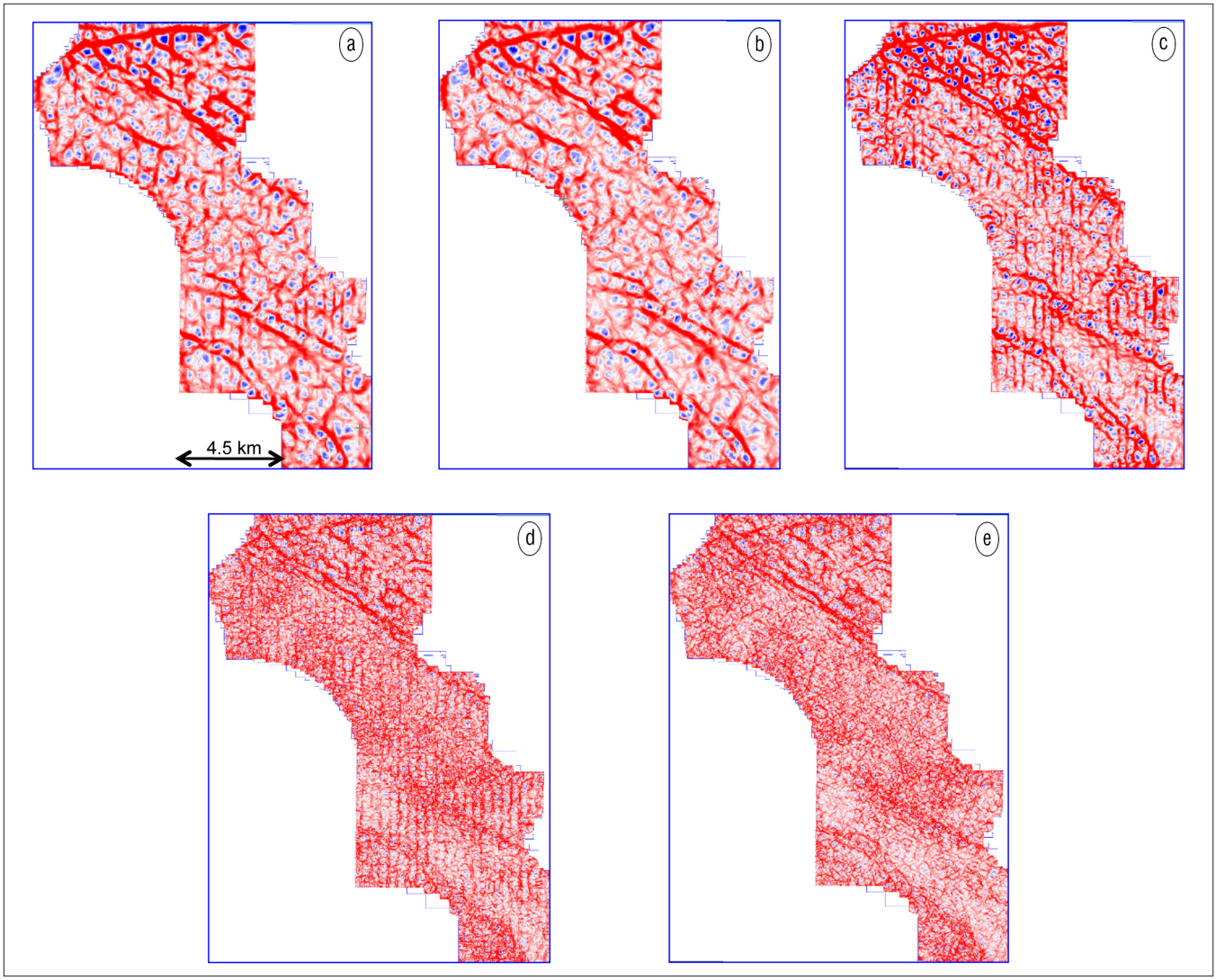

Figure 5. *Stratal slices from a most-positive curvature (long-wavelength) run on input seismic data; (b) most positive curvature (long-wavelength) run on input data after footprint filtering; (c) most-positive curvature (intermediate-wavelength) run on input seismic data; (d) most-positive curvature (short-wavelength) run on input seismic data; and (e) most-positive curvature (short-wavelength) run on input seismic data after footprint filtering.*

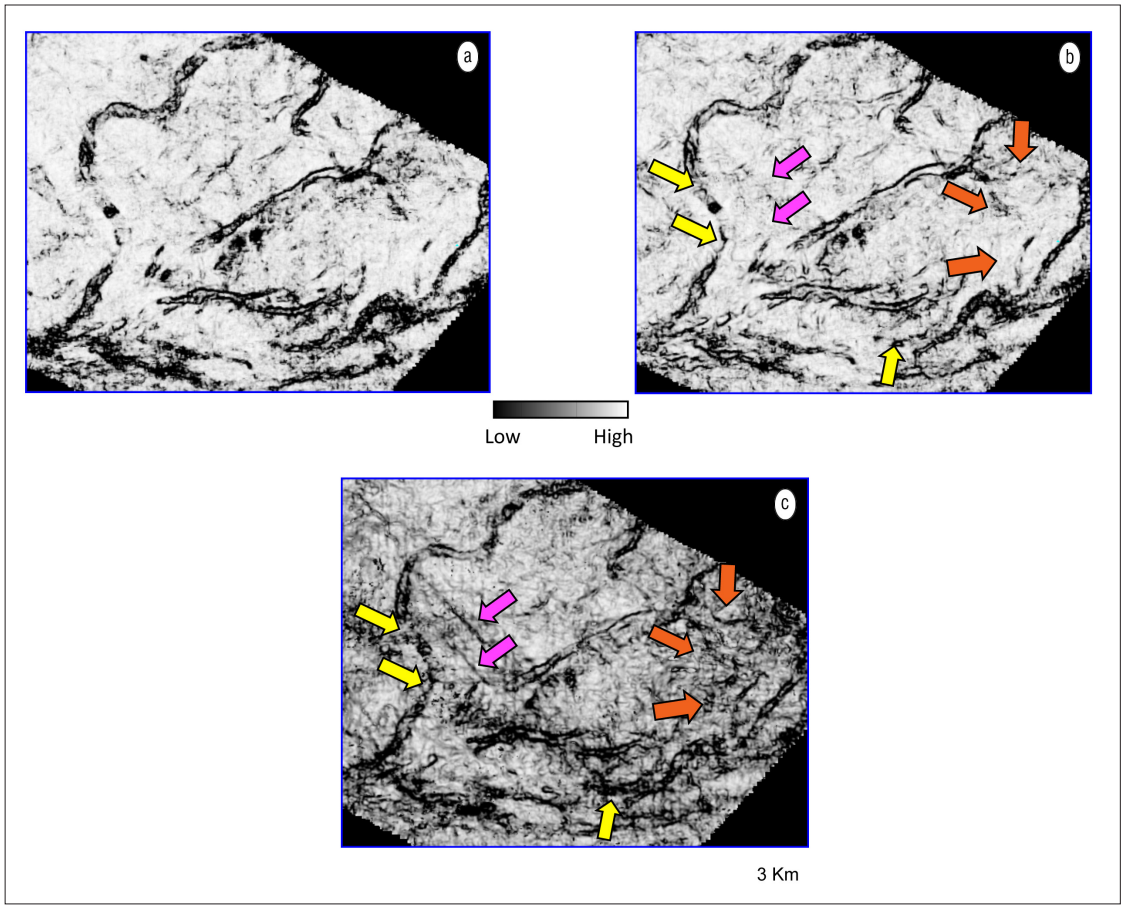

Figure 6. *Stratal slices from a coherence attribute run on (a) input seismic data, (b) input seismic data after time-variant spectral whitening, and (c) input data transformed to filtered thin-bed reflectivity inversion. Notice the improved image of stratigraphic features (orange and yellow block arrows) in (b) and (c) and subtle faults (magenta arrows) in (c).*

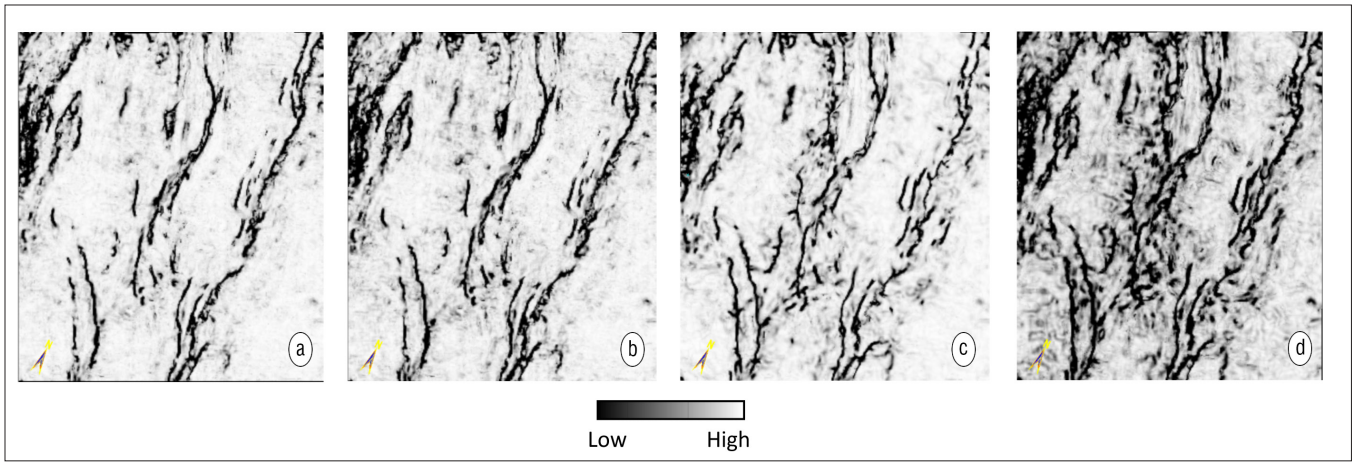

Figure 7. *Stratal slices from coherence attribute run on the (a) input data, as well as other frequency-enhanced seismic data such as (b) after Q-compensation (amplitude only), (c) time-variant spectral whitening, and (d) filtered thin-bed reflectivity inversion. Note that the coherence shows much more detail on the filtered thin-bed reflectivity version than the others.*

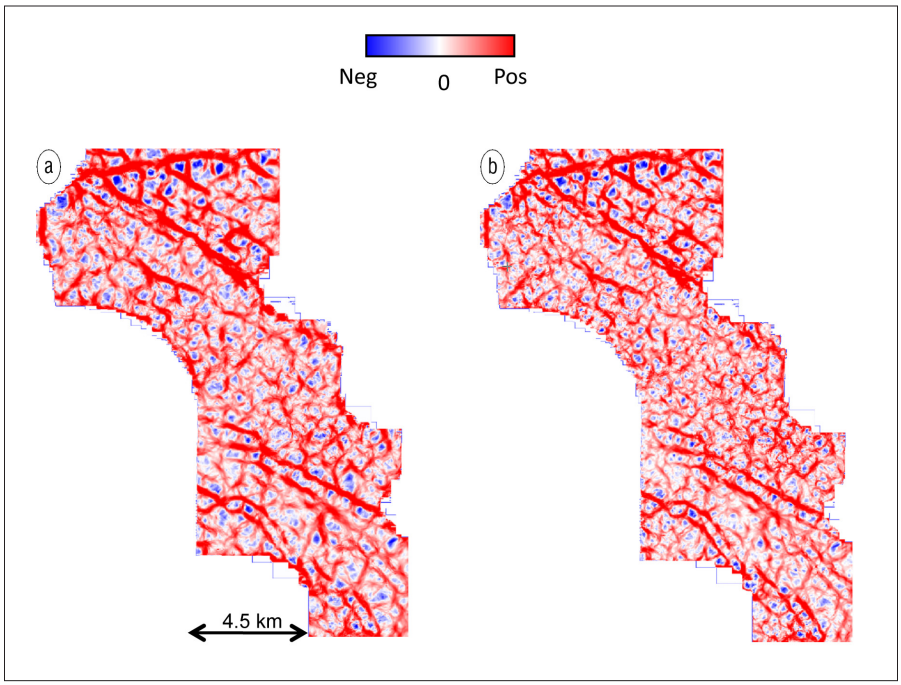

Figure 8. *Stratal slices from most-positive curvature run on (a) input seismic data after time-variant spectral whitening, and (b) input data transformed to filtered thin-bed reflectivity inversion. There is somewhat higher frequency on (b) as compared with (a) as the events look crisper. However, this difference is not as much as seen on the coherence attribute.*

thin reservoirs, these frequency-enhanced inverse images have proven useful in mapping subtle onlaps and offlaps, thereby facilitating the mapping of parasequences and the direction of sediment transport. Besides viewing the spectrally broadened seismic data in the form of reflectivity, it can be filtered back to any desired bandwidth that filter panel tests indicate, adding useful information for interpretational purposes.

Figure 3a compares a segment of a 5–80 Hz seismic section from Alberta and its thin-bed reflectivity inversion (Figure 3b). Notice the increased detail in terms of extra cycles. It is convenient for an interpreter to convolve the derived reflectivity volume with a 5–120 Hz band-pass wavelet that would yield a high-frequency volume. In addition to facilitating detailed interpretation, these filtered volumes can serve as input for generating high-bandwidth attribute volumes.

In Figure 4 we show a comparison of a seismic section and a time slice at t = 1140 ms before and after the application of time-variant spectral whitening and thin-bed reflectivity inversion. The amplitude spectrum for each data set is also shown. Notice that the high-frequency volume generated from thin-bed reflectivity inversion serves to show the highest frequency enhancement.

Attribute computation on preconditioned data

Whether it be random noise or acquisition footprint, application of one or more of the above data preconditioning methods result in attribute images that have improved vertical and lateral resolution and reduced contamination by artifacts, which we illustrate in the following examples.

Figure 5a shows a time slice at t = 1272 ms through a long-wavelength most-positive curvature attribute volume. Besides some oblique NW-SE trending lineaments that are geological, notice the NS imprint corresponding to the acquisition footprint. The equivalent slice from the intermediate-wavelength most-positive curvature (Figure 5b) exhibits even more pronounced footprint. As we go to short-wavelength most-positive curvature (Figure 5c), the footprint is seen even more pronounced such that we have low confidence in any lineament interpretation on this display.

In Figure 5d, we show the equivalent slice from the long-wavelength most-positive curvature run on the seismic data after footprint suppression. Notice the clean-looking display that does not show any artifact and so is amenable for more accurate interpretation. In Figure 5e, we show the equivalent slice from the most-positive curvature (short-wavelength) attribute computed on seismic data after footprint suppression.

In Figure 6, we show stratal slices through coherence volumes computed from the original seismic data as well as frequency-enhanced data generated using time-variant spectral whitening (Figure 6b) and filtered thin-bed reflectivity inversion (Figure 6c). Notice the significantly increased definition of channel features in Figures 6b and 6c, with the lateral resolution the best in Figure 6c. Due to this enhanced resolution, a faint acquisition imprint is also seen in Figure 6c.

Figure 7 shows stratal slices from coherence volumes run on (a) input data, (b) input data with inverse Q filtering, (c) spectrally whitened input data, and (d) input data transformed to filtered thin-bed reflectivity inversion. Notice that the coherence slices show increased resolution in the order stated above, with the highest lateral resolution seen for co-

herence computed on filtered thin-bed reflectivity inversion.

In Figure 8, we depict a suite of stratal slices through long-wavelength most-positive curvature volumes computed from (a) spectrally whitened data and (b) filtered thin-bed reflectivity. In this case, notice that unlike the coherence images shown in Figures 6c and 7d, the lateral resolution of the curvature images is only slightly enhanced in Figure 8b. Rather than being disappointing, the similarity of the curvature images confirms that broadening the spectrum does not significantly modify trace-to-trace relationships correlated to structure.

Conclusions

The motivation behind this work is to emphasize the fact that computation of attributes is definitely not just a process that involves pressing some buttons on a workstation, but requires careful examination of the input seismic data in terms of signal-to-noise ratio or any other noise contaminating the data as well as frequency content.

In our analysis we have compared the results for data before and after acquisition footprint filtered as well as different frequency enhancement of different frequency enhancement techniques like Q-compensation, spectral whitening, frequency-split structure-oriented filtering and thin-bed reflectivity inversion. We find that (1) attributes run on seismic data that have high signal-to-noise ratio or are processed for acquisition footprint suppression exhibits geological features clearly without any masking and so amenable for more accurate interpretation, and (2) that the enhancement in the frequency content for the data volumes analyzed is in the order they have been stated above. Needless to mention, all these methods may not be available to an interpreter. However, this exercise serves to bring out the information that should be borne in mind while making choices for methods of frequency enhancement. TLE

References

Chopra, S., J. Castagna, and O. Portniaguine, 2006, Seismic resolution and thin-bed reflectivity inversion: CSEG Recorder, no. 1, 19–25.

Chopra, S. and K. J. Marfurt, 2007, Seismic attributes for prospect identification and reservoir characterization: SEG.

Chopra, S. and K. J. Marfurt, 2008a, Emerging and future trends in seismic attributes: The Leading Edge, **27**, no. 3, 298–318, doi:10.1190/1.2896620.

Chopra, S. and K. J Marfurt, 2008b, Gleaning meaningful information from seismic attributes: First Break, 43–53.

Gulunay, N., N. Benjamin, and M. Magesan, 2006, Acquisition footprint suppression on 3D land surveys: First Break, **24**, no. 2, 71–77.

Helmore, S., 2009, Dealing with the noise—improving seismic whitening and seismic inversion workflows using frequency split structurally oriented filters: 79th Annual International Meeting, SEG, Expanded Abstracts, 3367–3371

Hoecker, C. and G. Fehmers, 2002, Fast structural interpretation with structure-oriented filtering: The Leading Edge, **21**, 238–243.

Luo, Y., S. Al-Dossary, and M. Alfaraj, 2002, Edge-preserving smoothing and applications: The Leading Edge, **21**, 136–158.

Marfurt, K. J., 2006, Robust estimates of dip and azimuth: Geophysics, **71**, no. 4, P29–P40.

Yilmaz, O., 2001, Seismic data analysis: SEG.

Acknowledgments: We thank Arcis Corporation for permission to present these results. Thin-bed reflectivity referred to in this article was derived using the commercial software called ThinMan™, a trademark owned by Fusion Petroleum Technologies, Houston.

Corresponding author: schopra@arcis.com